# Study of nuclei north-east or $^{48}$Ca with realistic effective hamiltonians

Luigi Coraggio

Istituto Nazionale di Fisica Nucleare - Sezione di Napoli

May, 21st 2012

- A. Covello (University of Naples and INFN)
- A. Gargano (INFN)
- N. Itaco (University of Naples and INFN)
- T. T. S. Kuo (SUNY at Stony Brook)
- L. C. (INFN)

# Why to study neutron-rich nuclei above doubly-closed $^{48}$Ca?

- To investigate the evolution of the spectroscopic properties of neutron-rich isotopic chains
- To ascertain if modern realistic shell-model potentials are able to reproduce the onset/disappearance of the $N = 40$ collectivity

# Why to study neutron-rich nuclei above doubly-closed $^{48}$Ca?

- To investigate the evolution of the spectroscopic properties of neutron-rich isotopic chains
- To ascertain if modern realistic shell-model potentials are able to reproduce the onset/disappearance of the $N = 40$ collectivity

*N. Itaco, L. C., A. Covello, and A. Gargano, J. Phys.: Conf. Ser.* **336**, *012008 (2011)*

# Excitation energies of the $J^\pi = 2_1^+$ states

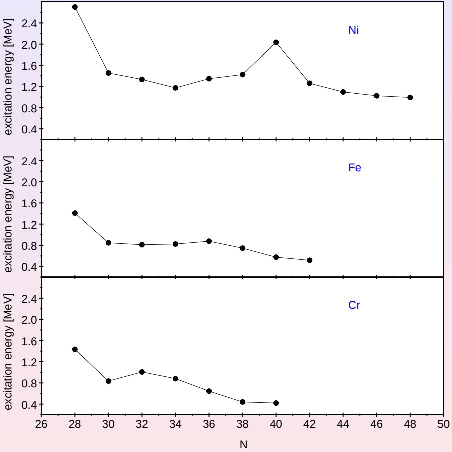


See for example A. Gade et al., Phys. Rev. C **81** 051304 (2010)

A main issue: what should be the shell-model hamiltonian to be employed for this calculation?

$$H = \sum_j \epsilon_j \hat{N}_j + \sum_{abcd} V_{abcd} a^\dagger_a a^\dagger_b a_c a_d$$

More precisely: what are the single-particle energies $\epsilon_j$ and the two-body matrix elements $V_{abcd}$ to be used?

A main issue: what should be the shell-model hamiltonian to be employed for this calculation?

$$H = \sum_j \epsilon_j \hat{N}_j + \sum_{abcd} V_{abcd} a^\dagger_a a^\dagger_b a_c a_d$$

More precisely: what are the single-particle energies $\epsilon_j$ and the two-body matrix elements $V_{abcd}$ to be used?

Common procedure: $\epsilon_j$ and $V_{abcd}$ are derived from the experimental data of the nuclei of the region under investigation, the drawback consists of a loss of predictive power

Microscopic approach (ours): we derive the shell-model hamiltonian from first principles, starting from realistic nucleon-nucleon forces

Common procedure: $\epsilon_j$ and $V_{abcd}$ are derived from the experimental data of the nuclei of the region under investigation, the drawback consists of a loss of predictive power

Microscopic approach (ours): we derive the shell-model hamiltonian from first principles, starting from realistic nucleon-nucleon forces

- First step: choose a realistic nucleon-nucleon potential and renormalize short-range correlations
- Second step: derive an effective shell-model hamiltonian $H_{\mathrm{eff}}$ by way of the many-body perturbation theory
- Third step: Diagonalize the shell-model hamiltonian in the chosen model space

(see L. C. *et al.*, Prog. Part. Nucl. Phys. **62** (2009) 135)

- First step: choose a realistic nucleon-nucleon potential and renormalize short-range correlations
- Second step: derive an effective shell-model hamiltonian $H_{\text{eff}}$ by way of the many-body perturbation theory
- Third step: Diagonalize the shell-model hamiltonian in the chosen model space

(see L. C. *et al.*, Prog. Part. Nucl. Phys. **62** (2009) 135)

- First step: choose a realistic nucleon-nucleon potential and renormalize short-range correlations
- Second step: derive an effective shell-model hamiltonian $H_{\rm eff}$ by way of the many-body perturbation theory
- Third step: Diagonalize the shell-model hamiltonian in the chosen model space

(see L. C. *et al.*, Prog. Part. Nucl. Phys. **62** (2009) 135)

- First step: choose a realistic nucleon-nucleon potential and renormalize short-range correlations
- Second step: derive an effective shell-model hamiltonian $H_{\rm eff}$ by way of the many-body perturbation theory
- Third step: Diagonalize the shell-model hamiltonian in the chosen model space

(see L. C. *et al.*, Prog. Part. Nucl. Phys. **62** (2009) 135)

# Phase 1: the realistic nucleon-nucleon potential

There are a plenty of $V_{NN}$s on the market: most of the modern ones reproduce quite well the physics of the two-nucleon system

The trouble with realistic $V_{NN}$s is the strong short-range repulsion

This is a notable shortcoming since we derive the shell-model effective hamiltonian from such potentials using the time-dependent degenerate linked-diagram perturbation theory

$$\Downarrow$$

It is necessary to handle the short-range repulsion

# Phase 1: the realistic nucleon-nucleon potential

There are a plenty of $V_{NN}$s on the market: most of the modern ones reproduce quite well the physics of the two-nucleon system

The trouble with realistic $V_{NN}$s is the strong short-range repulsion

This is a notable shortcoming since we derive the shell-model effective hamiltonian from such potentials using the time-dependent degenerate linked-diagram perturbation theory

$$\Downarrow$$

It is necessary to handle the short-range repulsion

# Phase 1: the realistic nucleon-nucleon potential

There are a plenty of $V_{NN}$s on the market: most of the modern ones reproduce quite well the physics of the two-nucleon system

The trouble with realistic $V_{NN}$s is the strong short-range repulsion

This is a notable shortcoming since we derive the shell-model effective hamiltonian from such potentials using the time-dependent degenerate linked-diagram perturbation theory

$$\Downarrow$$

It is necessary to handle the short-range repulsion

# Phase 1: the realistic nucleon-nucleon potential

There are a plenty of $V_{NN}$s on the market: most of the modern ones reproduce quite well the physics of the two-nucleon system

The trouble with realistic $V_{NN}$s is the strong short-range repulsion

This is a notable shortcoming since we derive the shell-model effective hamiltonian from such potentials using the time-dependent degenerate linked-diagram perturbation theory

$$\Downarrow$$

It is necessary to handle the short-range repulsion

# Phase 1: the realistic nucleon-nucleon potential

Old way: to resort to the calculation of the Brueckner $G$-matrix of the input $V_{NN}$ and use $G$-matrix vertices in the perturbative expansion of $H_{\rm eff}$

New approaches:

- to renormalize the $V_{NN}$ integrating out the high-momentum components of the potential - the $V_{\rm low-k}$ approach
- to employ a realistic potential derived from the chiral perturbation theory and defined only for low momenta - the so-called N$^3$LOW potential (see L.C., A. Covello, A. Gargano, N. Itaco, D. Entem, T. T. S. Kuo, and R. Machleidt, Phys. Rev. C **75** 024311 (2007))

# Phase 1: the realistic nucleon-nucleon potential

Old way: to resort to the calculation of the Brueckner $G$-matrix of the input $V_{NN}$ and use $G$-matrix vertices in the perturbative expansion of $H_{\mathrm{eff}}$

New approaches:

- to renormalize the $V_{NN}$ integrating out the high-momentum components of the potential - the $V_{\mathrm{low-k}}$ approach
- to employ a realistic potential derived from the chiral perturbation theory and defined only for low momenta - the so-called $N^3LOW$ potential (see L.C., A. Covello, A. Gargano, N. Itaco, D. Entem, T. T. S. Kuo, and R. Machleidt, Phys. Rev. C **75** 024311 (2007))

# Phase 2: the shell-model effective hamiltonian

A very useful way to derive $H_{\rm eff}$ is the time-dependent perturbative approach as developed by Kuo and his co-workers in the 1970s (see *T. T. S. Kuo and E. Osnes, Lecture Notes in Physics vol. 364 (1990)*)

In this approach the effective hamiltonian $H_{\rm eff}$ is expressed as

$$H_{\rm eff} = \hat{Q} - \hat{Q}' \int \hat{Q} + \hat{Q}' \int \hat{Q} \int \hat{Q} - \hat{Q}' \int \hat{Q} \int \hat{Q} \int \hat{Q} \cdots ,$$

- The integral sign represents a generalized folding operation (folded diagrams are summed up at all orders using Lee-Suzuki iterative technique)
- The $\hat{Q}$-box is a collection of irreducible valence-linked Goldstone diagrams that takes into account core-polarization effects for the valence nucleons in the model space

# Phase 2: the shell-model effective hamiltonian

A very useful way to derive $H_{\rm eff}$ is the time-dependent perturbative approach as developed by Kuo and his co-workers in the 1970s (see *T. T. S. Kuo and E. Osnes, Lecture Notes in Physics vol. 364 (1990)*)
In this approach the effective hamiltonian $H_{\rm eff}$ is expressed as

$$H_{\rm eff} = \hat{Q} - \hat{Q}' \int \hat{Q} + \hat{Q}' \int \hat{Q} \int \hat{Q} - \hat{Q}' \int \hat{Q} \int \hat{Q} \int \hat{Q} \cdots ,$$

- The integral sign represents a generalized folding operation (folded diagrams are summed up at all orders using Lee-Suzuki iterative technique)
- The $\hat{Q}$-box is a collection of irreducible valence-linked Goldstone diagrams that takes into account core-polarization effects for the valence nucleons in the model space

# Phase 2: the shell-model effective hamiltonian

A very useful way to derive $H_{\rm eff}$ is the time-dependent perturbative approach as developed by Kuo and his co-workers in the 1970s (see *T. T. S. Kuo and E. Osnes, Lecture Notes in Physics vol. 364 (1990)*)
In this approach the effective hamiltonian $H_{\rm eff}$ is expressed as

$$H_{\rm eff} = \hat{Q} - \hat{Q}' \int \hat{Q} + \hat{Q}' \int \hat{Q} \int \hat{Q} - \hat{Q}' \int \hat{Q} \int \hat{Q} \int \hat{Q} \cdots ,$$

- The integral sign represents a generalized folding operation (folded diagrams are summed up at all orders using Lee-Suzuki iterative technique)
- The $\hat{Q}$-box is a collection of irreducible valence-linked Goldstone diagrams that takes into account core-polarization effects for the valence nucleons in the model space

# Phase 2: the shell-model effective hamiltonian

$\hat{Q}$-box diagrams and all effective operators (electric quadrupole transitions, magnetic dipole transitions, ...) up to third order in perturbation theory.

We calculate the Padè approximant [2|1] of the $\hat{Q}$-box, in order to obtain a better estimate of the value to which the perturbation series should converge

$$[2|1] = V^0_{Qbox} + V^1_{Qbox} + V^2_{Qbox}(1 - (V^2_{Qbox})^{-1} V^3_{Qbox})^{-1} \quad ,$$

We include enough intermediate states so that the $H_{\rm eff}$ has a flat dependence on them

# Phase 2: the shell-model effective hamiltonian

$\hat{Q}$-box diagrams and all effective operators (electric quadrupole transitions, magnetic dipole transitions, ...) up to third order in perturbation theory.

We calculate the Padè approximant [2|1] of the $\hat{Q}$-box, in order to obtain a better estimate of the value to which the perturbation series should converge

$$[2|1] = V^0_{Qbox} + V^1_{Qbox} + V^2_{Qbox}(1 - (V^2_{Qbox})^{-1} V^3_{Qbox})^{-1} \quad ,$$

We include enough intermediate states so that the $H_{\mathrm{eff}}$ has a flat dependence on them

# Phase 2: the shell-model effective hamiltonian

$\hat{Q}$-box diagrams and all effective operators (electric quadrupole transitions, magnetic dipole transitions, ...) up to third order in perturbation theory.

We calculate the Padè approximant [2|1] of the $\hat{Q}$-box, in order to obtain a better estimate of the value to which the perturbation series should converge

$$[2|1] = V^0_{Qbox} + V^1_{Qbox} + V^2_{Qbox}(1 - (V^2_{Qbox})^{-1} V^3_{Qbox})^{-1} \quad ,$$

We include enough intermediate states so that the $H_{\rm eff}$ has a flat dependence on them

# Phase 2: the shell-model effective hamiltonian

In our calculations we include also a certain class of diagrams that are usually neglected: the so-called self-consistency corrections




The sum at all orders of this class of diagrams makes results independent from the choice of the unperturbed hamiltonian $H_0 = T + U = \sum_i (p_i^2/2M + M\omega^2 r_i^2/2)$ and is equivalent to employ a Hartree-Fock basis

# Phase 2: the shell-model effective hamiltonian

In our calculations we include also a certain class of diagrams that are usually neglected: the so-called self-consistency corrections

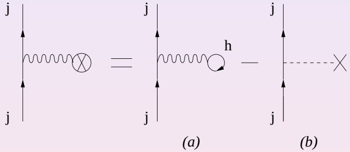


The sum at all orders of this class of diagrams makes results independent from the choice of the unperturbed hamiltonian $H_0 = T + U = \sum_i (p_i^2/2M + M\omega^2 r_i^2/2)$ and is equivalent to employ a Hartree-Fock basis

# Phase 2: the shell-model effective hamiltonian

In our calculations we include also a certain class of diagrams that are usually neglected: the so-called self-consistency corrections

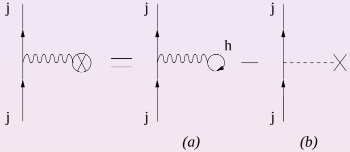


The sum at all orders of this class of diagrams makes results independent from the choice of the unperturbed hamiltonian $H_0 = T + U = \sum_i (p_i^2/2M + M\omega^2 r_i^2/2)$ and is equivalent to employ a Hartree-Fock basis

# $\hat{Q}$-box perturbative expansion: 1-body diagrams

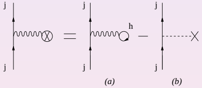


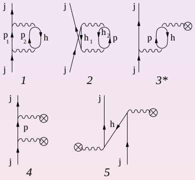


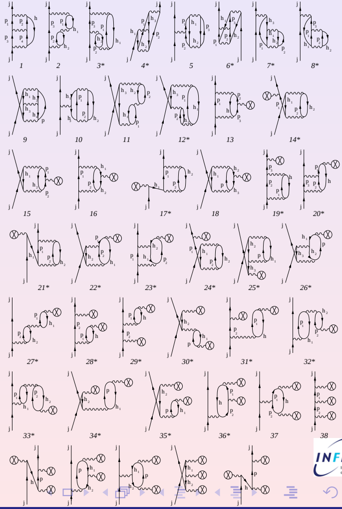

# $\hat{Q}$-box perturbative expansion: 2-body diagrams

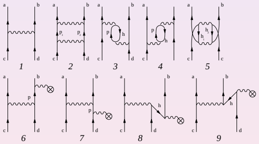

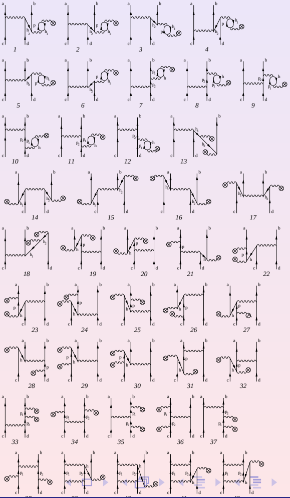

# $\hat{Q}$-box perturbative expansion: 2-body diagrams

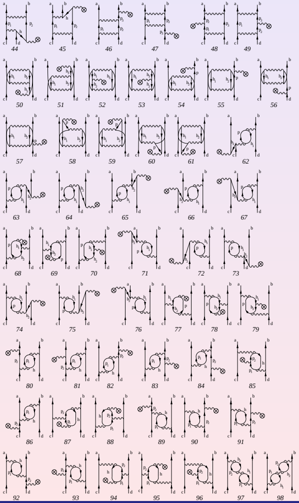

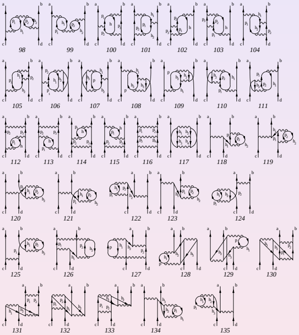

*L.C., A. Covello, A. Gargano, N. Itaco, and T. T. S. Kuo, to be published in Annals of Physics (2012)*

# Test: $^6$Li first excited states with N$^3$LO potential

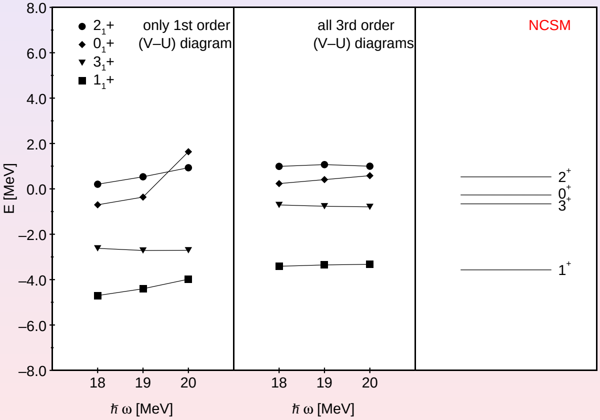

# Phase 3: the diagonalization of the shell-model hamiltonian

- Input $V_{NN}$: we derive a $V_{\mathrm{low-k}}$ with a cutoff momentum $\Lambda = 2.6\ \mathrm{fm}^{-1}$ from the high-precision *NN* CD-Bonn potential.
- We consider $^{48}$Ca a closed core, our chosen model space is spanned by the four neutron SP orbitals $2p_{3/2}$, $2p_{1/2}$, $1f_{5/2}$, $0g_{9/2}$ and proton SP orbital $1f_{7/2}$.
- We derive $H_{\mathrm{eff}}$ calculating the Padè approximant [2|1] of the $\hat{Q}$-box.
- We employ as single-particle energies both the theoretical one and those obtained from the spectrum of the first excited states of $^{49}$Ca and $^{49}$Sc.

# Phase 3: the diagonalization of the shell-model hamiltonian

- Input $V_{NN}$: we derive a $V_{\rm low-k}$ with a cutoff momentum $\Lambda = 2.6~{\rm fm}^{-1}$ from the high-precision *NN* CD-Bonn potential.
- We consider $^{48}$Ca a closed core, our chosen model space is spanned by the four neutron SP orbitals $2p_{3/2},~2p_{1/2},~1f_{5/2},~0g_{9/2}$ and proton SP orbital $1f_{7/2}$.
- We derive $H_{\rm eff}$ calculating the Padè approximant [2|1] of the $\hat{Q}$-box.
- We employ as single-particle energies both the theoretical one and those obtained from the spectrum of the first excited states of $^{49}$Ca and $^{49}$Sc.

# Phase 3: the diagonalization of the shell-model hamiltonian

- Input $V_{NN}$: we derive a $V_{\rm low-k}$ with a cutoff momentum $\Lambda = 2.6~\rm fm^{-1}$ from the high-precision *NN* CD-Bonn potential.
- We consider $^{48}$Ca a closed core, our chosen model space is spanned by the four neutron SP orbitals $2p_{3/2},~2p_{1/2},~1f_{5/2},~0g_{9/2}$ and proton SP orbital $1f_{7/2}$.
- We derive $H_{\rm eff}$ calculating the Padè approximant [2|1] of the $\hat{Q}$-box.
- We employ as single-particle energies both the theoretical one and those obtained from the spectrum of the first excited states of $^{49}$Ca and $^{49}$Sc.

# Phase 3: the diagonalization of the shell-model hamiltonian

- Input $V_{NN}$: we derive a $V_{\rm low-k}$ with a cutoff momentum $\Lambda = 2.6 \ {\rm fm}^{-1}$ from the high-precision *NN* CD-Bonn potential.
- We consider $^{48}$Ca a closed core, our chosen model space is spanned by the four neutron SP orbitals $2p_{3/2}, \ 2p_{1/2}, \ 1f_{5/2}, \ 0g_{9/2}$ and proton SP orbital $1f_{7/2}$.
- We derive $H_{\rm eff}$ calculating the Padè approximant [2|1] of the $\hat{Q}$-box.
- We employ as single-particle energies both the theoretical one and those obtained from the spectrum of the first excited states of $^{49}$Ca and $^{49}$Sc.

# Convergence properties of theoretical SP energies and TBME

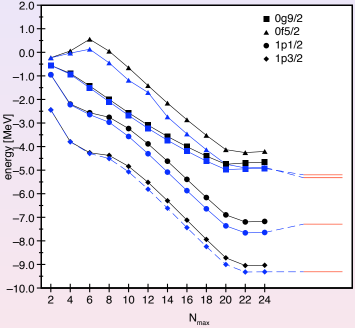


- Black squares: third-order calculation
- Blue squares: Padè [2,1] calculation
- Red spectrum: experimental data

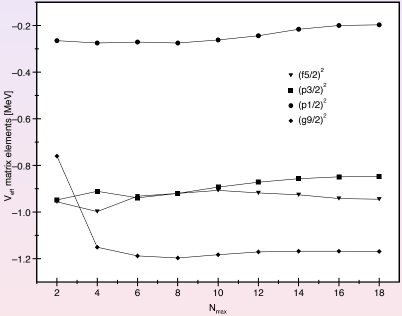

# Results: the heavy calcium isotopes

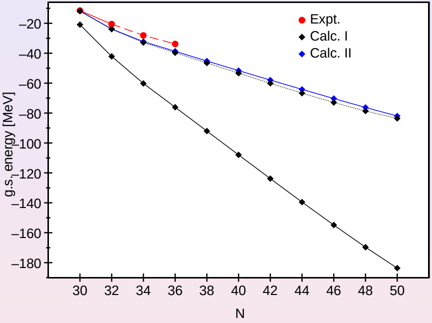


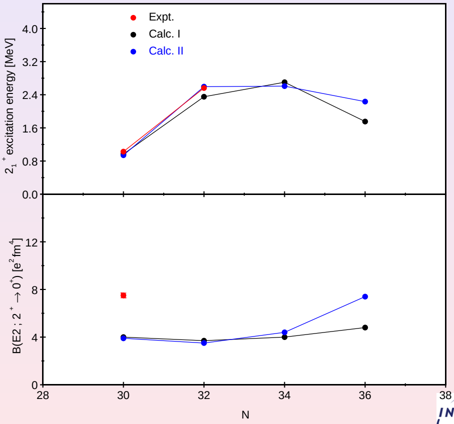


- Black diamonds: theoretical SP energies
- Blue diamonds: experimental SP energies
- Red dots: experimental data

# Results: the titanium isotopes

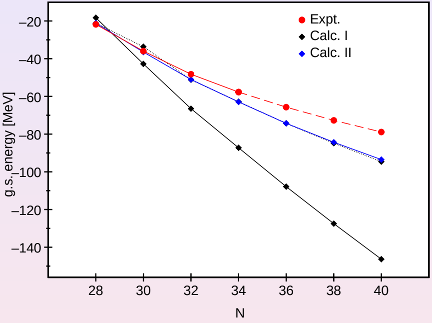


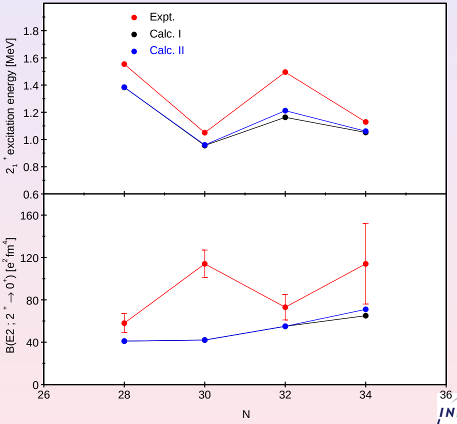


- Black diamonds: theoretical SP energies
- Blue diamonds: experimental SP energies
- Red dots: experimental data

# Results: the chromium isotopes

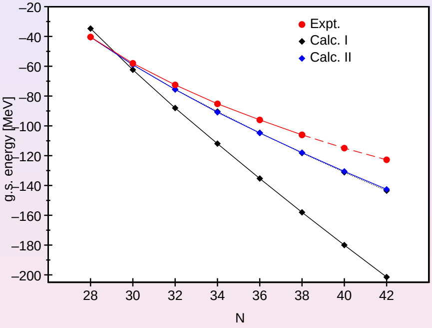


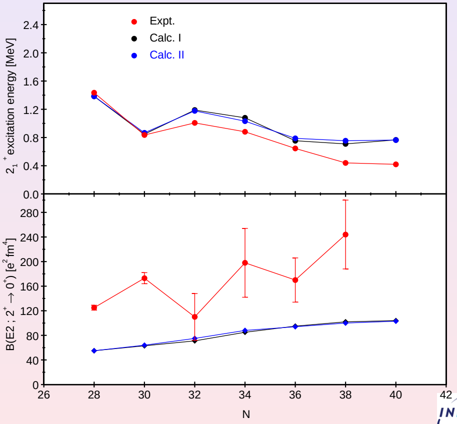


- Black diamonds: theoretical SP energies
- Blue diamonds: experimental SP energies
- Red dots: experimental data

# Results: the iron isotopes

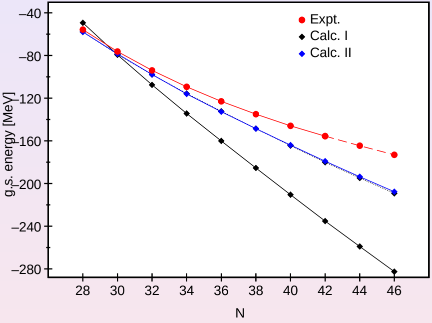


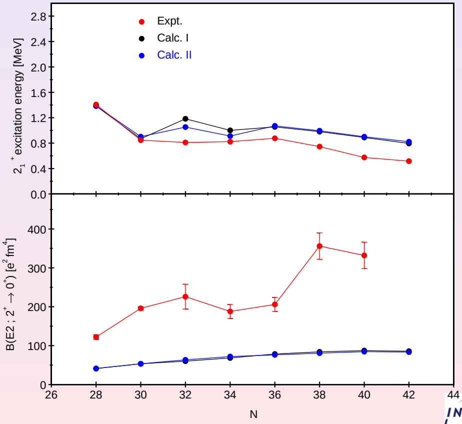


- Black diamonds: theoretical SP energies
- Blue diamonds: experimental SP energies
- Red dots: experimental data

# Results: the nickel isotopes

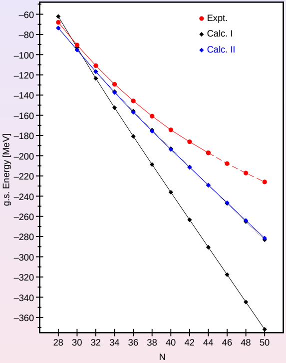


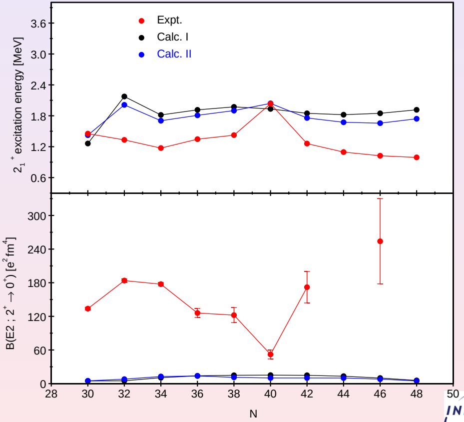


- Black diamonds: theoretical SP energies
- Blue diamonds: experimental SP energies
- Red dots: experimental data

# Main remarks

- The agreement of our results with many experimental data testifies the reliability of our $V_{\text{eff}}$
- No need of $T = 1$ monopole corrections
- However, we fail to reproduce the onset of collectivity at $N = 40$
- Need to enlarge the neutron model space? (see S. M. Lenzi *et al.*, Phys. Rev. C **82** (2010) 054301)

# Main remarks

- The agreement of our results with many experimental data testifies the reliability of our $V_{\mathrm{eff}}$
- No need of $T = 1$ monopole corrections
- However, we fail to reproduce the onset of collectivity at $N = 40$
- Need to enlarge the neutron model space? (see S. M. Lenzi *et al.*, Phys. Rev. C **82** (2010) 054301)

# Main remarks

- The agreement of our results with many experimental data testifies the reliability of our $V_{\mathrm{eff}}$
- No need of $T = 1$ monopole corrections
- However, we fail to reproduce the onset of collectivity at $N = 40$
- Need to enlarge the neutron model space? (see S. M. Lenzi *et al.*, Phys. Rev. C **82** (2010) 054301)

# Main remarks

- The agreement of our results with many experimental data testifies the reliability of our $V_{\mathrm{eff}}$
- No need of $T = 1$ monopole corrections
- However, we fail to reproduce the onset of collectivity at $N = 40$
- Need to enlarge the neutron model space? (see S. M. Lenzi *et al.*, Phys. Rev. C **82** (2010) 054301)

# Results including $\nu 1d_{5/2}$ orbital in the model space

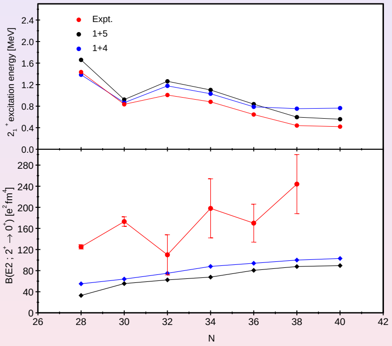


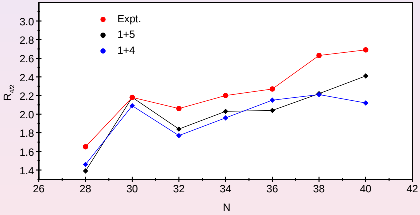


Chromium isotopes

# Results including $\nu 1d_{5/2}$ orbital in the model space

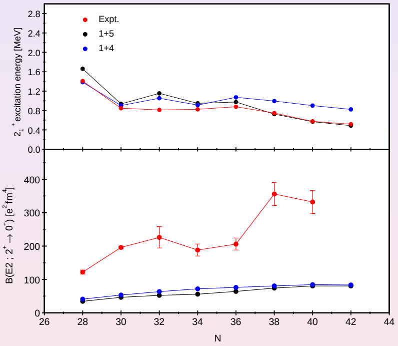


Iron isotopes

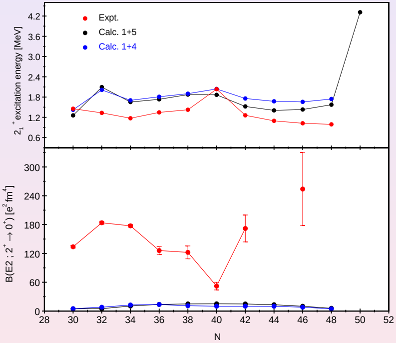


Nickel isotopes

# Results including $\pi 1p_{3/2}$ and $\nu 1d_{5/2}$ orbital in the model space

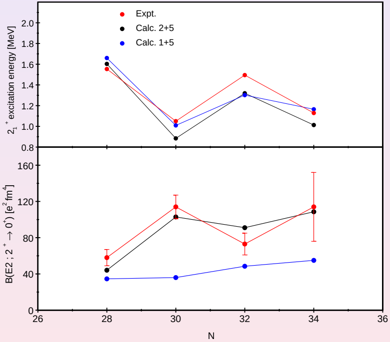


Titanium isotopes

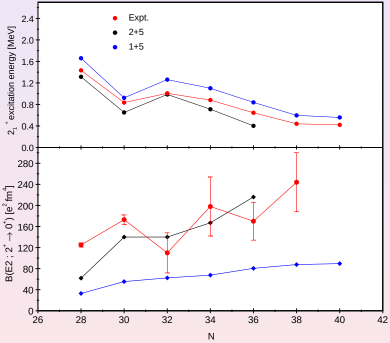


Chromium isotopes

# Results including $\pi 1p_{3/2}$ and $\nu 1d_{5/2}$ orbital in the model space

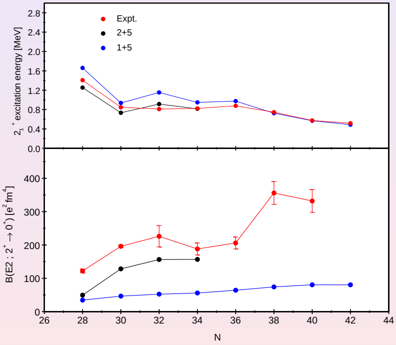


Iron isotopes

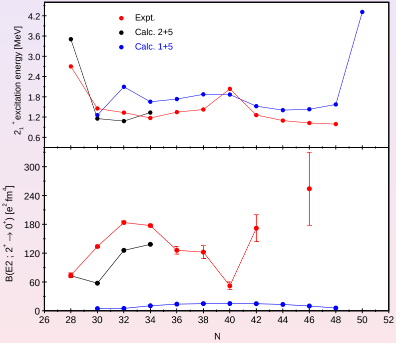


Nickel isotopes